Acta Crystallographica Section D
Biological Crystallography
ISSN 0907-4449

Crystal engineering yields crystals of cyclophilin D diffracting to 1.7 Å resolution

Daniel Schlatter,* Ralf Thoma, Erich Küng, Martine Stihle, Francis Müller, Edilio Borroni, Andrea Cesura‡ and Michael Hennig*

F. Hoffmann–La Roche Ltd, Pharmaceutical Research Discovery, CH-4070 Basel, Switzerland

‡ Current address: Evotec NeuroSciences, August-Forel Strasse 1, CH-8008 Zürich, Switzerland.

Correspondence e-mail: daniel.schlatter@roche.com, michael.hennig@roche.com

Received 11 November 2004
Accepted 27 January 2005

PDB References: cyclophilin D, 2bit, r2bitsf; DMSO complex, 2biu, r2biusf.

In the pharmaceutical industry, knowledge of the three-dimensional structure of a specific target facilitates the drug-discovery process. Despite possessing favoured analytical properties such as high purity and monodispersion in light scattering, some proteins are not capable of forming crystals suitable for X-ray analysis. Cyclophilin D, an isoform of cyclophilin that is expressed in the mitochondria, was selected as a drug target for the treatment of cardiac disorders. As the wild-type enzyme defied all attempts at crystallization, protein engineering on the enzyme surface was performed. The K133I mutant gave crystals that diffracted to 1.7 Å resolution using in-house X-ray facilities and were suitable for soaking experiments. The crystals were very robust and diffraction was maintained after soaking in 25% DMSO solution: excellent conditions for the rapid analysis of complex structures including crystallographic fragment screening.

1. Introduction

Cyclophilins form a ubiquitous family of proteins characterized by their ability to catalyze *cis–trans* isomerization of peptidylprolyl bonds. Catalysis of nascent protein folding is one of the presumed functions of cyclophilins (Galat, 1993). The immunosuppressive drug cyclosporin A (CsA) binds to cyclophilins and strongly inhibits their isomerase activity at nanomolar concentrations (Kallen *et al.*, 1998). The mitochondrial isoform of this enzyme is termed cyclophilin D (CypD). There is evidence that CypD has an additional function in the regulation of the permeability of the transition pore in mitochondria (Halestrap *et al.*, 2002). The pore is formed from a complex of the voltage-dependent anion channel, the adenine nucleotide translocase and CypD at the contact sites between the mitochondrial outer and inner membrane. Uncontrolled opening of the pore leads to loss of matrix volume control, uncouples mitochondrial energy transduction and would compromise cell viability. Therefore, pore activation is thought to be a critical event in the induction of apoptotic cell death, an important topic of research in many disease areas. Further evidence of the involvement of CypD in mitochondrial membrane permeabilization was deduced by CsA-inhibition experiments that showed pore opening to be independent of the immunosuppressant properties of CsA (Brenner *et al.*, 2003). Therefore, inhibition of CypD is a potential treatment for neuronal and cardiac disorders (Mattson & Kroemer, 2003).

In order to support drug discovery with relevant structural information, a high-resolution X-ray crystallographic system for the study of protein–ligand complexes is advantageous. To date, three structures of mammalian cyclophilins, namely

CypA, CypB and CypC, are known (Bergsma *et al.*, 1991). Alignment of the amino-acid sequences shows that they share a significant degree of identity (75% for CypA, 60% for CypB and 57% for CypC as calculated for the region of sequence overlap), but depending on their individual localization in the cell they all have different N-terminal extensions (Fig. 1). In the present study, we describe the cloning and expression of cyclophilin D in *Escherichia coli*, its purification and crystallization. As the wild-type protein could not be crystallized, several strategies including construct engineering and site-directed mutagenesis were applied in order to improve the crystallization properties of CypD.

Site-directed mutagenesis for crystal engineering was applied for the first time more than a decade ago (Lawson *et al.*, 1991; McElroy *et al.*, 1992). In the hope that sequence modifications on the surface of a particular protein recalcitrant to crystallization may improve its biochemical properties or may introduce favourable crystal contacts, exchanges of single and multiple amino-acid residues were performed. Although from time to time promising results have been published, the lack of specific rules for the mutagenesis strategy has prevented the method being applied generally. Recently, a series of studies showing examples of mutational surface engineering that facilitated protein crystallization were reported (Czepas *et al.*, 2004; Derewenda *et al.*, 2004; Longenecker *et al.*, 2001; Mateja *et al.*, 2002). It was demonstrated that mutation of charged residues, preferably lysine and glutamate to alanine or lysine to arginine, could improve the crystallization properties of the proteins significantly. For cyclophilin D, we designed target specific mutants geared to the homology to other cyclophilins and the unusually high p*K* and solubility properties of the protein. The K133I single mutant changed the crystallization properties of the protein drastically so that crystals with diffraction to 1.7 Å resolution could be obtained and used for structural analysis.

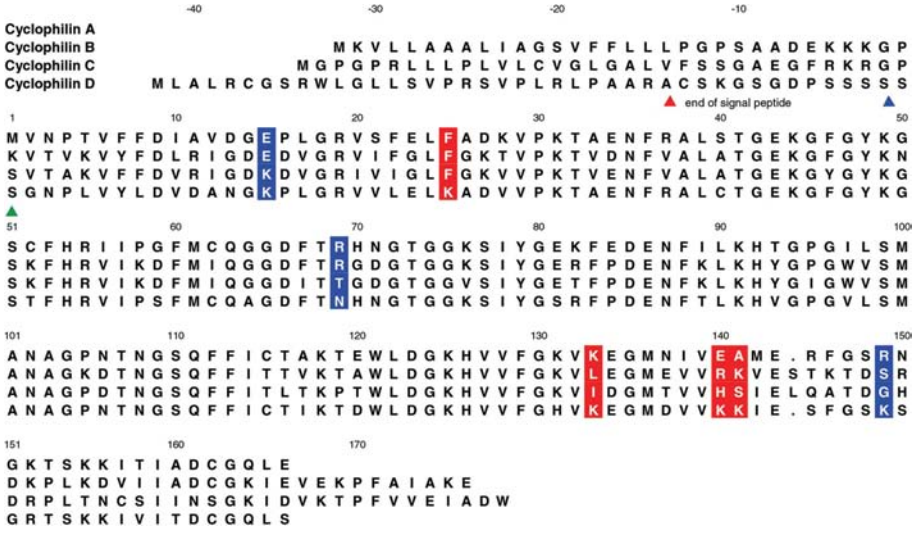

Figure 1
Sequence alignment of several isoforms of cyclophilin. The sequences were numbered according to cyclophilin A. The red triangle highlights the position of the end of the signal peptide that guides translocation into the mitochondria. The blue triangle marks the cleavage site of subtilisin in the protease screen. The green triangle indicates the first amino acid of the construct that was used for the production of tCypD, tCypD/K133I and all other mutated proteins. Please note that cyclophilin D corresponds to the SWISS-PROT entry ppif_human (named cyclophilin F therein).

2. Materials and methods

2.1. DNA manipulation and sequence analysis

Standard protocols for preparation of DNA probes, digestion with restriction endonucleases, DNA ligation and transformation of *E. coli* strains were used. For DNA sequencing, the ABI PRISM BigDye Terminator Cycle Sequencing Ready Reaction Kit v.1.1 and ABI PRISM 310 Genetic Analyzer was used. PCRs were performed in a T3 Thermocycler (Whatman Biometra) using *Pfu* polymerase (Stratagene).

2.2. Cloning

The human cyclophilin D gene was amplified by PCR using the plasmid pET15b-CypDΔ29 (starting at Cys−13 and cloned *Bam*HI/*Bam*HI). The oligonucleotides CYPDu1, 5′-CTCGAG**CATATG**TGCAGCAAGGG-3′, and CYPDu2, 5′-CCTCC**CATATG**GGGAAC CCGCTCGTG-3′, with an *Nde*I site (in bold) were used as 5′-primers to construct two truncated versions of CypD starting at Cys−13 (CypDΔ29) and Gly2 (tCypD) (codons for these amino acids are underlined), respectively. Furthermore, the primers included an artificial translation-initiation (Met) codon as part of the restriction site *Nde*I. As 3′-primer, the oligonucleotide CYPDl, 5′-CGGGCTTTGTTAGCAGCCGG-3′, was used. Using the new *Nde*I and the existing *Bam*HI restriction site, the amplified DNA fragment was cloned into the expression plasmid pET21a to yield the plasmids pET21a-CypDΔ29 and pET21a-tCypD without any tag. The integrity of the constructs was confirmed by DNA sequencing.

2.3. Mutagenesis

Point mutations were introduced into the tCypD gene with the QuikChange site-directed mutagenesis kit (Stratagene), using the plasmid pET21a-tCypD as template. Mutagenesis was carried out as described in the protocol supplied with the kit. The following oligonucleotides and their complementary counterparts were used (newly introduced restriction sites for the control of the reaction are in bold and base substitutions to introduce an amino-acid exchange are underlined): 5′-GGA CGC CAA CGG GGA GCC GCT CGG CCG CG-3′ for construction of tCypD/K15E, 5′-GGG GGC GAC TTC **ACG CGT** CAC AAT GGC ACA GGC GG-3′ (*Mlu*I site introduced) for tCypD/N69R, 5′-GAA TCT TTC GGC **TCT AGA** AGT GGG AGG ACA TCC AAG AAG-3′ (*Xba*I site introduced) for tCypD/K149R, 5′-CCG CGT GGT

GCT GGA GCT GTT CGC AGA TGT CGT CCC-3′ for tCypD/K25F, 5′-CGG TCA CGT CAT TGA GGG CAT GGA CGT CG-3′ for tCypD/K133I, 5′-GGG CAT GGA CGT CGT GGA GAA AAT AGA ATC TTT CGG C-3′ for tCypD/K140E, 5′-GGG CAT GGA CGT CGT GAA GGC AAT AGA ATC TTT CGG C-3′ for tCypD/K141A and 5′-GGG CAT GGA CGT CGT GGA GGC AAT AGA ATC TTT CGG C-3′ for tCypD/140E/K141A.

2.4. Purifcation of tCypD and variants

Expression was conducted in *E. coli* BL21(DE3) cells. Two 2 l flasks with 1 l LB medium were inoculated with an overnight culture of freshly transformed cells supplemented with 0.1 mg ml^{-1} ampicillin. The culture was incubated at 303 K and overexpression was induced at an optical density at 600 nm (OD_{600}) of 0.6 by adding IPTG to a final concentration of 1 m*M*. After another 6 h of incubation, the culture reached an OD_{600} of 2.5 and the cells were harvested by centrifugation (Sorvall RC-3B, 4000 rev min^{-1}, 30 min, 277 K) and stored at 253 K. About 3.5 g cells (wet weight) were obtained per litre of culture.

Cells were resuspended in 100 m*M* Tris–HCl pH 7.8, 2 m*M* EDTA, 1 m*M* TCEP (buffer *A*) containing one Complete protease-inhibitor cocktail tablet (Roche Diagnostics AG, Switzerland) per 50 ml buffer and were lysed with a French press at 60 MPa. The supernatant of the centrifuged homogenate (Beckman JA-20, 48 000*g*, 1 h, 277 K) was applied to a column of EMD COO^- equilibrated with buffer *A*. The column was washed with equilibrium buffer and bound proteins were eluted with five column volumes of a linear gradient from 0 to 500 m*M* NaCl. The combined peak fractions were dialyzed against buffer *A* and loaded onto a Q-Sepharose column equlibrated with buffer *A*. Almost pure tCypD was collected in the flowthrough fraction. The protein solution was concentrated in a Ultrafree-15 ultrafiltration device (Millipore) and further fractionated on a column of EMD BioSeq (1.6 × 60 cm), eluting with 50 m*M* potassium phosphate buffer pH 7.3, 2 m*M* EDTA, 1 m*M* TCEP, 100 m*M* NaCl.

3 mg tCypD was obtained per gram of wet cell mass. SDS polyacrylamide analysis as well as chromatography on a protein-C4 reverse-phase column (Vydac) using 0.1% TFA/0.08% TFA in acetonitrile showed pure protein (>95%). The protein had a monodisperse size distribution when analyzed by analytical ultracentifugation (Beckman Optima XL-A) and dynamic light scattering (Protein Solutions DynaPro). Concentration was determined from the UV absorbance at 280 nm using a calculated extinction coefficient $\varepsilon_{280} = 9965\ M^{-1}\ cm^{-1}$.

2.5. Peptidylprolyl *cis–trans* isomerase (PPI) assay

The enzymatic activities of the wild-type and mutated cyclophilins were measured according to Kofron *et al.* (1991*a*,*b*) with minor modifications. The assay was carried out in 96-well microplates (black plate with clear bottom, Costar) and the reaction was monitored by use of a POLARstar Galaxy microplate reader (BMG Labtechnologies GmbH, Offenburg, Germany) kept in a fridge at 277 K. The following reagents were added to each well: 42 µl 100 m*M* NaCl in 50 m*M* HEPES pH 8 and 100 µl recombinant cyclophilin D (final concentration 24 n*M*). The microplate was then placed in the microplate reader and allowed to equilibrate at 277 K for 15 min. At time zero, 7 µl peptide substrate, *N*-Suc-AAPF-*p*-nitroaniline (Bachem, Switzerland) dissolved in anhydrous 2,2,2-trifluorethanol containing 470 m*M* LiCl, was injected into the well. 1 s later, 100 µl chymotrypsin (final concentration 175 units ml^{-1}) was added and the *cis–trans* isomerization of the peptide substrate was monitored by measuring the absorbance (405 nm) of the cleaved *p*-nitroaniline. Absorbance readings taken in the time interval from 3 to 7 s after the addition of the peptide substrate were used to estimate the initial velocity of the reaction. In order to measure the spontaneous isomerization rate of the peptide substrate, the addition of cyclophilin D was omitted in some wells and substituted by the addition of HEPES buffer.

2.6. Determination of pI

Determination of the isoelectric point (pI) was performed by isoelectric focusing on IsoGel agarose IEF plates pH 3–10 (FMC BioProducts Europe, Denmark) following the instruction manual. The proteins were applied to precast gels and dialyzed against 1% glycerol. The anolyte was 0.5 *M* acetic acid pH 2.6 and the catholyte was 1 *M* NaOH pH 13. IEF Marker 3-10 (Serva Electrophoresis GmbH, Germany) was used as a standard.

2.7. Fluorescence titration

Fluorescence measurements were performed on a SLM-AMINCO 8100 double-grating spectrofluorometer by adding a known concentration of cyclosporin A to the protein solution. The intrinsic fluorescence of cyclophilin D was excited through its single tryptophan (Trp121) at 280 nm and was detected at 340 nm. The protein concentration was 200 n*M* in 10 m*M* HEPES buffer pH 7.4 containing 150 m*M* NaCl.

The intensity was corrected for protein dilution and filter effect according to Birdsall *et al.* (1983). The corrected fluorescence intensity was plotted against ligand concentration and fitted by a sigmoidal function from which the dissociation constant K_d was computed according to the law of mass action under the assumption of formation of a 1:1 protein–ligand complex (Eftink, 1997).

2.8. Crystallization

For crystallization experiments, the enzyme was prepared in a solution with about 31 mg ml^{-1} protein concentration in 50 m*M* potassium/sodium phosphate pH 7.3, 100 m*M* NaCl, 2 m*M* EDTA and a Roche screening set of 94 crystallization conditions was used to test the crystallization ability of the corresponding mutants. No crystals suitable for X-ray investigation were observed for tCypD or any mutant enzymes apart from tCypD/K133I.

Table 1
Statistics of X-ray data collection and refinement.

Values in parentheses are for the last shell.

	Apo	DMSO
Space group	$P4_12_12$	$P4_12_12$
Unit-cell parameters (Å)	$a = b = 57.17$, $c = 87.23$	$a = b = 57.02$, $c = 87.64$
Temperature (K)	120	120
Measured reflections	91268	48970
Unique reflections	16168	15197
Resolution range (Å)	15.0–1.71 (1.82–1.71)	15.0–1.71 (1.82–1.71)
Completeness (%)	99.2 (98.5)	98.4 (94.7)
R_{sym}†	0.046 (0.138)	0.056 (0.093)
No. of protein atoms	1239	1239
No. of water molecules	392	339
No. of ligand atoms	0	15
R.m.s. distances (Å)	0.008	0.009
R.m.s. bond angles (°)	1.1	1.2
R_{work}‡, end refinement (%)	13.9	14.8
R_{free}, end refinement (5% of data) (%)	17.5	18.5
Mean B factor, protein (Å^2)	10.1	9.7
Mean B factor, ligand (Å^2)	—	27.5
Mean B factor, solvent (Å^2)	26.9	28.3

† $R_{sym} = \sum_{hkl}\sum_i |I(hkl)_i - \langle I(hkl)\rangle| / \sum_{hkl}\sum_i I(hkl)_i$. ‡ R factor $= \sum |F(hkl)_o - F(hkl)_c| / \sum F(hkl)_o$.

tCypD/K133I crystallized under a wide range of conditions. Using the vapour-diffusion method in hanging drops at room temperature, the protein solution was mixed with an equal volume of the reservoir solution with 30% Jeffamine in HEPES pH 7.0. Well formed single crystals appeared within a few days and grew to maximum dimensions of 0.3 × 0.3 × 0.2 mm. The crystal of the DMSO complex was produced by soaking of a crystal in the crystallization buffer with 25% DMSO for 30 min.

2.9. X-ray and structure analysis

The crystals were mounted in cryo-loops directly from the drop and flash-frozen using liquid nitrogen. Subsequently, the crystals were analyzed using a rotating-anode generator (50 mA, 40 kV) as X-ray source and a MAR Research image-plate area detector (300 mm). Information on data collection is summarized in Table 1. Data were processed using *DENZO* (Otwinowski, 1993) and scaled using the *CCP*4 (Collaborative Computational Project, Number 4, 1994) suite of programs.

Molecular-replacement computations were carried out with *AMoRe* (Navaza, 1994) using cyclophilin A (PDB code 1swj) as a search model. The top solution gave a correlation coefficient of 35.2 and an R factor of 50.4%, which fell to 35.3% after rigid-body refinement. Refinement was performed using *ARP*/*wARP* followed by a few cycles of manual rebuilding using *MOLOC* (Gerber, 1992) and refinement with *REFMAC* (Murshudov *et al.*, 1999). The final model of the enzyme contains all residues of the protein from Gly2 to Ser165.

Calculation of the surface area was performed using the program *XSAE* (C. Broger, personal communication) with a probe radius of 1.4 Å.

Table 2
Mutants of tCypD.

All protein preparations were analyzed by analytical ultracentrifugation and dynamic light scattering. No significant quality difference with respect to monodispersity was observed.

Mutant	Reason for mutation	Result
K15E	Reduce number of lysines, shift pI of protein Glu15 forms crystal contact in cyclophilin A	No crystals
N69R	Introduce arginine Arg69 forms crystal contact in cyclophilin A	No crystals
K149R	Reduce number of lysines and introduce arginine Arg149 forms crystal contact in cyclophilin A	No crystals
K25F	Reduce number of lysines, shift pI and lower solubility of protein Phe25 in cyclophilins A, B and C	No crystals
K140E	Reduce number of lysines, shift pI of protein Glu140 in cyclophilin A	No crystals
K141A	Reduce number of lysines, shift pI and lower solubility of protein Ala141 in cyclophilin A	No crystals
K140E and K141A	Reduce number of lysines, shift pI of protein	No crystals
K133I	Reduce number of lysines, shift pI and lower solubility of protein Ile133 in cyclophilin C	Crystals

3. Results and discussion

3.1. Protein engineering for crystallization

As several crystal structures of isoforms of cyclophilin have previously been analyzed at high resolution, the crystallization and structure determination of cyclophilin D was initially considered to be straightforward. The starting point was CypDΔ29, expressed and purified with an N-terminal 6×His tag which was successfully used in the biological assay including high-throughput screening, as the construct without 6×His tag was not expressed by *E. coli*. Light-scattering experiments on the protein showed aggregation and no crystals could be grown. Nevertheless, we used this protein for a protease-digestion screening and sequence analysis of one of the fragments obtained upon cleavage with subtilisin resulted in a stable core protein that lacked the 41 N-terminal residues (Fig. 1). The cleavage site was found to be between Ser−2 and Ser−1, close to the first residue of the core protein. Based on this data and sequence homology to cyclophilin A (75% similarity), a new construct was selected that is two amino acids shorter compared with the core protein obtained upon cleavage with subtilisin and starts with Gly2 (tCypD). Owing to cloning limitations, a methionine was added to the N-terminus. After optimization of expression and purification, a yield of approximately 3 mg of pure protein per gram of wet cells could be obtained for analysis of function and crystallization behaviour. The protein was highly active in the isomerase assay and showed monodispersion in analytical ultracentrifugation and dynamic light scattering. Although the likelihood of crystallization should be high for such proteins (D'Arcy, 1994), screening of several hundred crystallization conditions failed to produce any crystals.

Based on this optimized system of protein expression and purification, several single-amino-acid mutations were intro-

duced in order to alter the protein's properties (Table 2). The selection of the mutations was guided by a number of different considerations. Generally, only amino acids located at a secure distance from the active site were taken into account for site-directed mutagenesis. Following experience with other proteins, we mostly altered lysine residues, the least favoured residue in crystal contacts, to other residue types (Dasgupta *et al.*, 1997). In contrast to the lysine-to-alanine mutation strategy (Derewenda, 2004), we introduced amino-acid residues such as glutamic acid, phenylalanine and isoleucine to specifically modify the protein with respect to other biochemical properties. With some of our mutations we tried to reintroduce specific crystal contacts that exist in the known crystal structure of cyclophilin A. Reducing the pI of the protein by replacing positively charged lysines with negatively charged glutamic acids or other amino acids found at this position in other cyclophilin variants was another strategy. Cyclophilin D exhibits a very high isoelectric point, experimentally determined to be 10.2 (Table 3), that originates from 20 positively and 15 negatively charged residues (compared with 20 positively and 19 negatively charged residues in cyclophilin A). In addition to lowering the pI, we aimed at reducing the solubility of tCypD by introducing hydrophobic residues. At 40 mg ml^{-1} protein in crystallization buffer, the solubility of tCypD is exceptionally high.

It is interesting to note that all but one of the mutations resulted in no improvement with regard to crystallization. Only the single mutant tCypD/K133I immediately gave crystals of exceptionally good quality (Fig. 2*a*). X-ray analysis of the crystals shows tetragonal symmetry and high-resolution diffraction that enabled rapid data collection. The exceptional stability of the crystals is demonstrated by their resistance to extreme soaking conditions in 25% DMSO without significant loss of diffraction quality (Fig. 2*b*).

As the main goal of this project was the use of the X-ray analysis for structure-based design, functional analyses of tCypD and mutated tCypD/K133I were performed (Table 3). Firstly, the peptidylprolyl *cis–trans* isomerase (PPI) assay gave very similar enzyme substrate turnover rates indicating functional integrity. Secondly, a fluorescence titration experiment was performed to prove the binding capability of the enzyme (Fig. 3). Binding of cyclosporin A to cyclophilin D resulted in fluorescence enhancement owing to water shielding of Trp121 and very similar binding constants can be calculated (Table 3).

The experimentally determined isoelectric point (pI) for the mutant tCypD/K133I is 9.5, in good agreement with the purpose of the mutation to reduce the pI compared with the wild-type protein.

3.2. Crystal structure of cyclophilin D

Using high-quality and high-resolution diffraction data, the structure determination of cyclophilin D was straightforward (for details, see §1). The fold of cyclophilin D is essentially identical to that of other cyclophilins (r.m.s.d. of C^{α} positions 0.5 Å^2; Fig. 4). A detailed analysis of the active-site geometry and comparison to cyclophilin A shows only minor differences.

Table 3
Biochemical properties of tCypD and mutant tCypD/K133I.

	tCypD	tCypD/K133I
Peptidylprolyl isomerase activity/ substrate turnover (nmol s^{-1})	5.8	6.2
Binding constant K_d of cyclosporin A binding (n*M*)	12.5	13.7
Isoelectric point pI	10.2	9.5

Inspection of the crystal packing identified one prominent crystal contact. It is formed by Ile133, Leu5, Val21, Leu164, Glu23 and Glu134 of one molecule and by the side chains of Tyr79, Pro84, Ser81, Asn106 and several backbone atoms of the residues between Ser79 and Pro84 as well as Asn106 of the neighbouring molecule (Fig. 5). Overall, 772 Å^2 surface area is covered by this contact with mainly hydrophobic properties (510 Å^2). The hydrophobic cluster is shielded against the solvent by more hydrophilic residues, including at least five direct intermolecular hydrogen bonds between Glu23 and Ser81, His131 and the carbonyl of Tyr79, Ser165 and the carbonyl of Asn106 and the carbonyl of Leu164 and the side chain of Asn106. In addition, several water-mediated hydrogen bonds are observed. The location and environment of the mutation Ile133 proves that this crystal contact would not be possible in the wild-type protein because of steric clashes as well as the positive charge of the Lys residue. Beside the crystal contact that includes Ile133, no further crystal contact is present that could contribute to the very good stability of this crystal system.

3.3. Crystal structure with DMSO

Frequently, the solubility of substances for complex structure determination is rather low and the addition of DMSO is required to obtain a suitable ligand concentration. In order to prove the robustness of the crystals towards soaking in DMSO solutions, a 25% DMSO solution was prepared and the crystals soaked for 30 min. Subsequently, a crystal was flash-frozen in liquid nitrogen and data collection performed. Data analysis showed a minor reduction in diffraction quality compared with untreated crystals and refinement to 1.7 Å resolution was straightforward. The protein structures with and without DMSO treatment are essentially identical apart from the localization of at least four DMSO molecules. Two of the molecules are located in the active site of the enzyme (Fig. 6). In addition to hydrophobic interactions, the oxide of molecule DMSO-1 is at a hydrogen-bonding distance to Arg55 (distance 2.8 Å) and the oxide of DMSO-2 is at a distance of 3 Å from the backbone amide of Asn102. This is evidence that key interactions that have been identified in the interaction of cyclophilin A with cyclosporin A are also important for the design of ligands for cyclophilin D. Crystal robustness as shown with this soaking experiment is instrumental in fragment-based X-ray screening.

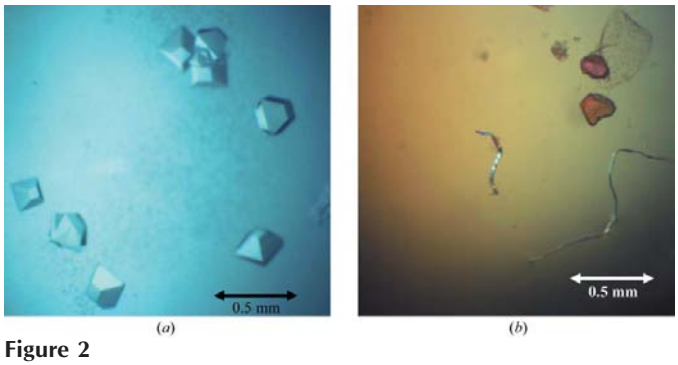

Figure 2
Crystals of tCypD/K133I produced as described in §2. The mutant protein crystallized under a wide range of different conditions. (*a*) Examples of crystals grown in the course of the initial crystallization screening and (*b*) after 30 min soaking of the same crystals in 25% DMSO.

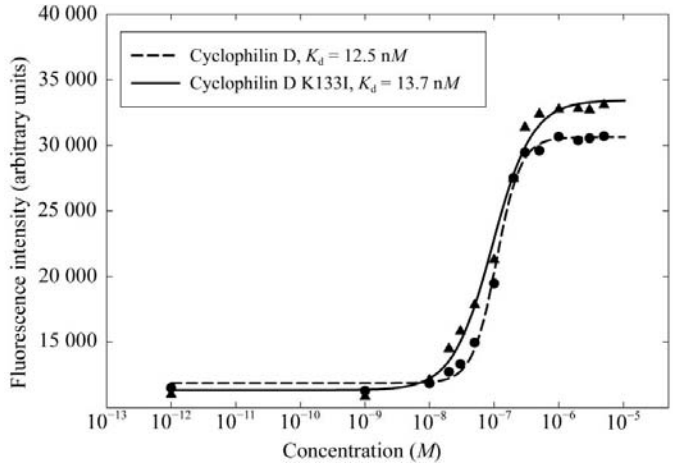

Figure 3
Fluorescence titration of cyclosporin A binding to tCypD. Upon binding of CsA to the cyclophilin, tryptophan emission of the single Trp121 increases. Fluorescence titration was performed by adding small aliquots of a known ligand concentration to the protein solution and measuring the fluorescence intensity. A plot of the corrected fluorescence intensities *versus* ligand concentration is fitted by a sigmoidal function. The dissociation constant K_d is computed according to the law of mass action. 1:1 binding is assumed.

4. Conclusions

Crystal engineering was essential to obtain crystals for high-resolution X-ray analysis of cyclophilin D. This promising result shows that a single mutant can alter a protein significantly to enable the formation of a crystal contact that would be impossible with the wild-type protein. The strong hydrophobic interaction, facilitated by Ile133, represents the key crystal contact and together with the high symmetry of the crystals ($P4_12_12$) a stable network of intermolecular interaction can be observed. It is obvious that rational design of such interactions is not possible even if crystal structures of highly homologous proteins are available.

The lack of specific guidelines on how to alter a protein's surface is a large hurdle for the wider application of crystal engineering. A rational surface-engineering protocol was established by Derewenda (2004). Some examples suggest that the method of Lys substitution by Ala on the surface is a promising approach that reduces the high conformational entropy of lysine side chains. This has the advantage of giving a relatively clear guideline, but in most cases two to three substitutions clustered together at the surface are required to obtain crystals that diffract well. Modelling the replacement of Lys133 by Ala in the crystal contact shows that the crystal contact could still be formed, but appears to be less optimal since the hydrophobic interaction formed by the Ile side chain could no longer be achieved. Since there are multiple ways to make a protein amenable to crystallization, we believe that our approach of altering protein properties offers another route to explore for the planning of surface mutations. Substitution of solvent-exposed surface residues such as lysine with non-alanine residues found in homologous proteins has the advantage of having a high probability of being tolerated in the scaffold at this position. To a great extent, the selection of amino-acid replacements is a trial-and-error procedure, but this example shows that improvements in crystallization properties are possible with rather a small number of mutations. The number of variants required for success is compatible with efforts that can reasonably be invested to determine a crystal structure. In this respect, cyclophilin D represents a favourable application of crystal engineering, but demonstrates that considerable effort and time is required for this method to be successful.

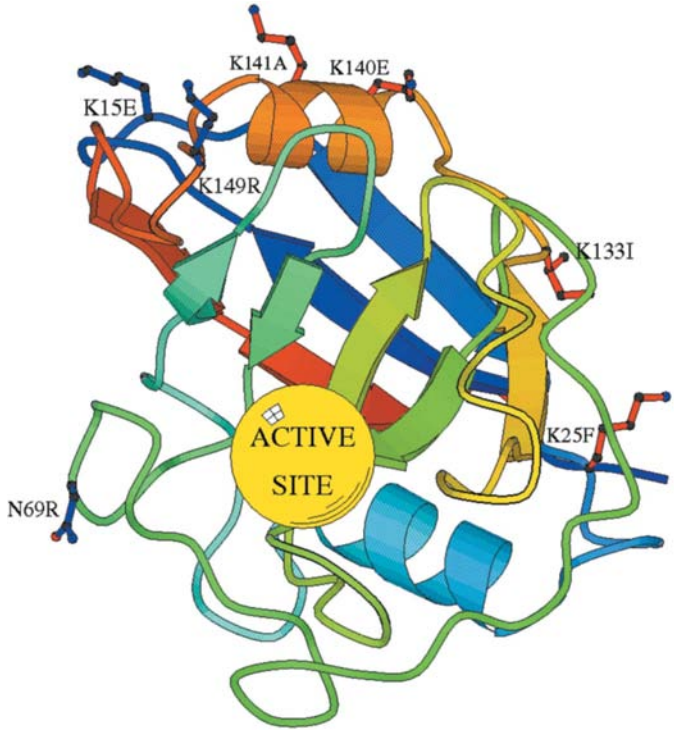

Figure 4
Ribbon representation of tCypD. The positions of the site-directed mutations made to facilitate crystallization are highlighted in ball-and-stick representation. All are located on the surface of the protein and distant from its active site in order to avoid any interference with the activity of the enzyme. Only the protein with mutation K133I could successfully be crystallized. At this position isoleucine is depicted, whereas all other highlighted amino acids are from the 'wild-type' sequence.

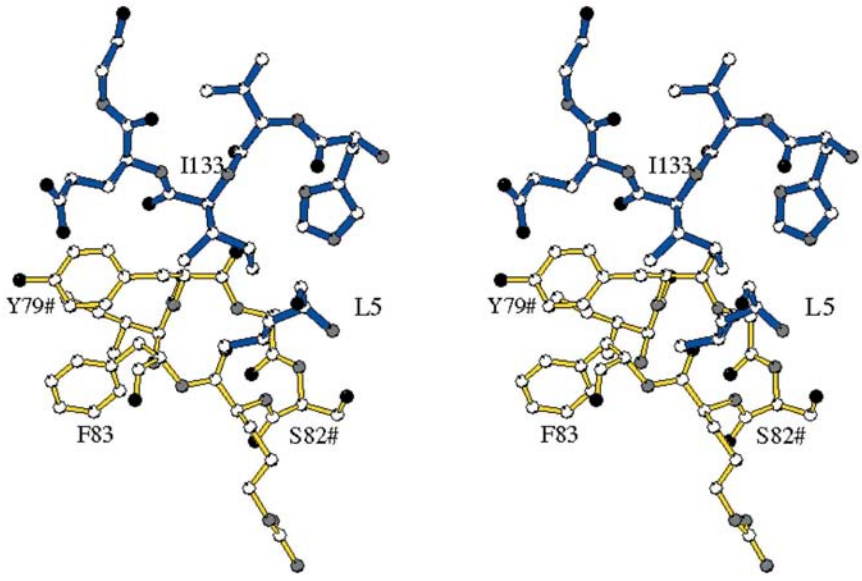

Figure 5
(*a*) Stereoview in ball-and-stick representation with sticks coloured blue and yellow for the molecules that form the crystal contact. The mutation K133I favors the formation of the crystal contact with mainly hydrophobic interactions. A lysine side chain at this position would cause steric clashes and disable this crystal packing.

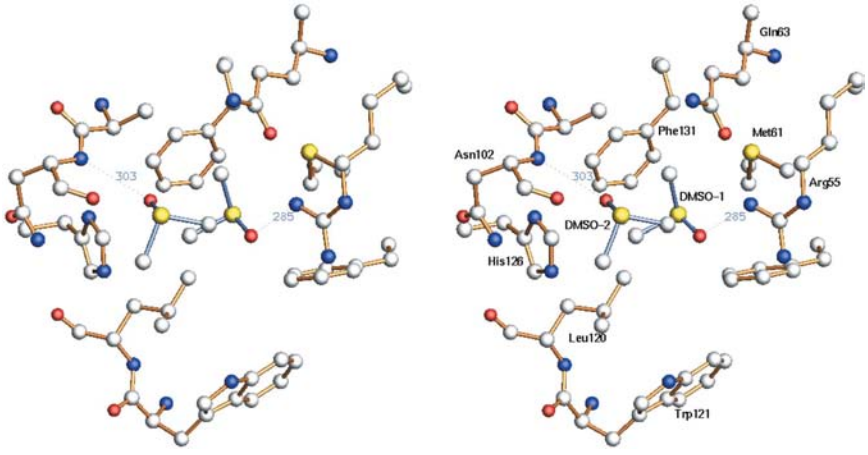

Figure 6
Soaking with 25% DMSO resulted in four DMSO-binding sites with very high confidence. Two DMSO molecules were identified in close proximity to the active site of the enzyme. DMSO-1 forms a hydrogen bond to the guanidine group of Arg55 and DMSO-2 forms a hydrogen bond to Asn102 NH, a hydrogen bond that is also formed in the complex of cyclophilin A with cyclosporin A.

We thank Glenn E. Dale for helpful discussions at the beginning of this project and Allan D'Arcy for help with the protease digest. For their skilful technical assistance in protein characterization, we thank Patricia Glaentzlin and Eric Kusznir. Furthermore, we thank Jeremy Beauchamp for critical reading of the manuscript.

References

Bergsma, D. J., Eder, C., Gross, M., Kersten, H., Sylvester, D., Appelbaum, E., Cusimano, D., Livi, G. P., McLaughlin, M. M., Kasyan, K., Porter, T. G., Silverman, C., Dunnington, D., Hand, A., Prichett, W. P., Bossard, M. J., Brandt, M. & Levy, M. A. (1991). *J. Biol. Chem.* **266**, 23204–23214.

Birdsall, B., King, R. W., Wheeler, M. R., Lewis, C. A. Jr, Goode, S. R., Dunlap, R. B. & Roberts, G. C. K. (1983). *Anal. Biochem.* **132**, 353–361.

Brenner, C., Le Bras, M. & Kroemer, G. (2003). *J. Clin. Immunol.* **23**, 73–80.

Collaborative Computational Project, Number 4 (1994). *Acta Cryst.* D**50**, 760–763.

Czepas, J., Devedjiev, Y., Krowarsch, D., Derewenda, U., Otlewski, J. & Derewenda, Z. S. (2004). *Acta Cryst.* D**60**, 275–280.

D'Arcy, A. (1994). *Acta Cryst.* D**50**, 469–471.

Dasgupta, S., Iyer, G. H., Bryant, S. H., Lawrence, C. E. & Bell, J. A. (1997). *Proteins Struct. Funct. Genet.* **28**, 494–514.

Derewenda, U., Mateja, A., Devedjiev, Y., Routzahn, K. M., Evdokimov, A. G., Derewenda, Z. S. & Waugh, D. S. (2004). *Structure*, **12**, 301–306.

Derewenda, Z. S. (2004). *Structure*, **12**, 529–535.

Eftink, M. R. (1997). *Methods Enzymol.* **278**, 258–286.

Galat, A. (1993). *Eur. J. Biochem.* **216**, 689–707.

Gerber, P. R. (1992). *Biopolymers*, **32**, 1003–1017.

Halestrap, A. P., McStay, G. P. & Clarke, S. (2002). *J. Biochimie*, **84**, 153–166.

Kallen, J., Mikol, V., Taylor, P. & Walkinshaw, M. D. (1998). *J. Mol. Biol.* **283**, 435–449.

Kofron, J. L., Kuzmic, P., Kishore, V., Colon-Bonilla, E. & Rich, D. H. (1991*a*). *Biochemistry*, **30**, 6127–6134.

Kofron, J. L., Kuzmic, P., Kishore, V., Colon-Bonilla, E. & Rich, D. H. (1991*b*). *Biochemistry*, **30**, 10818.

Lawson, D. M., Artymiuk, P. J., Yewdall, S. J., Smith, J. M. A., Livingstone, J. C., Treffry, A., Luzzago, A., Levi, S., Arosio, P., Cesareni, G., Thomas, C. D., Shaw, W. V. & Harrison, P. M. (1991). *Nature (London)*, **349**, 541–544.

Longenecker, K. L., Garrard, S. M., Sheffield, P. J. & Derewenda, Z. S. (2001). *Acta Cryst.* D**57**, 679–688.

McElroy, H. E., Sisson, G. W., Schoettlin, W. E., Aust, R. M. & Villafranca, J. E. (1992). *J. Cryst. Growth*, **122**, 265–272.

Mateja, A., Devedjiev, Y., Krowarsch, D., Longenecker, K., Dauter, Z., Otlewski, J. & Derewenda, Z. S. (2002). *Acta Cryst.* D**58**, 1983–1991.

Mattson, M. P. & Kroemer, G. (2003). *Trends Mol. Med.* **9**, 196–205.

Murshudov, G. N., Vagin, A. A., Lebedev, A., Wilson, K. S. & Dodson, E. J. (1999). *Acta Cryst.* D**55**, 247–255.

Navaza, J. (1994). *Acta Cryst.* A**50**, 157–163.

Otwinowski, Z. (1993). *Proceedings of the CCP4 Study Weekend: Data Collection and Processing*, edited by L. Sawyer, N. Isaacs & S. Bailey, pp. 56–62. Warrington: Daresbury Laboratory.